Optimization of volumetric error calibration procedures based on a digital twin

B. Iñigo1, N. Colinas-Armijo1, G. Aguirre1, L.N. López de Lacalle2
[1]*Design and Precision Engineering Group, IDEKO, 20870 Elgoibar, Basque Country, Spain*
[2]*Department of Mechanical Engineering, EHU-UPV, 48013 Bilbao, Basque Country, Spain*

Abstract

Following the Industry 4.0 trend, real time monitoring systems have become a crucial element for machine tool manufacturers in order to monitor the state of the machine during its whole lifetime. Concerning the field of machine errors and volumetric accuracy, automatic or semi-automatic measurement systems that can be integrated in the machine are becoming of major importance, in order to perform fast machine calibration and verification procedures. Repeating such measurements frequently allows the user and/or the manufacturer to monitor the volumetric performance of the machine on a day to day basis and take the corresponding preventive actions without affecting the production.

In order to implement a measurement system in every machine and to use it periodically, measurement time and equipment cost are critical in these applications. The approach presented in this work is based on measuring calibrated artefacts within the working volume and extracting the required information on the accuracy of the machine.

Due to the necessity of optimizing different aspects, a Digital-Twin based calibration and compensation procedure is presented. Several aspects of the calibration and compensation process are optimized in order to find the best measurement strategy for each application according to volumetric performance-based criteria. A 3-axis moving-column type milling machine is selected as case study. The resulting calibration strategy represents a cost and time effective procedure that can be integrated in a machine.

1 Introduction

Volumetric accuracy in machine tools was defined as the ability of the machine to produce accurate 3D shapes [1]. The development of volumetric error mapping

strategies, and the compensation of the measured systematic errors, has been the focus of many research projects over the time [2].

There is a trend towards the integration of self-diagnosis systems in machine tools following *Industry 4.0* principles, and the verification and recalibration of volumetric accuracy is one of the key requirements. Artefact based calibration systems find here an important advantage due to their much lower cost compared to laser tracker-based solutions, and they are therefore a reasonable alternative to explore.

In [3] a virtual calibration and compensation procedure was presented, capable to simulate the whole process in order to optimize different aspects of the procedure. This document is presented as a continuation of the this work, but a different approach is used in the modelling of the errors of the virtual machine. A cantilever-type travelling column 3-axis milling machine will be taken as the case study, calibrated with a 1D ball array. Details of the machine are given next.

Kinematic chain: Tool-Y-Z-X-Bed-Workpiece

Workspace (mm): X(0-4000), Z(0-1500), Y(0-1300)

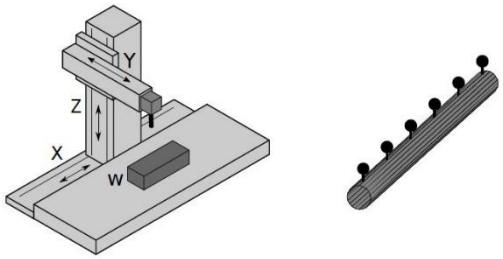

Figure 1. (left) Machine kinematic structure; (right) 1D ball array

2 Virtual optimization of the error mapping procedure

The general structure of the virtual error mapping and compensation procedure was presented in [3]. The process is divided in 3 main stages: error mapping test, model estimation and validation test. Two Digital Twins of the machine are used in order to simulate the original machine measured and the compensation model obtained. Additional details of the modelling of these digital twins are given in section 3.

3 Digital twin of the machine tool

As mentioned in section 1, cantilever-type travelling column 3-axis milling machine with a large working volume will be taken as the case study. Two digital twins of the machine are required in the implementation of the virtual error mapping procedure. The machine model M is the one to be calibrated and can include as many effects as needed to be considered in the analysis, as the compensation model C is the one used to predict the machine behaviour.

The virtual machine models *VM* provide the position of the tool centre point (TCP) in the machine's main coordinate system, in function of the programmed axis positions *X(x, y, z)*, the tool offset *t*, and any other effect that may deviate it, such as guiding errors, backlash, thermal effects, etc., which are parameterized in the model by a set of parameters *E*.

$$\begin{cases} M = VM(X, t, E_M) \\ C = VM(X, t, E_c) \end{cases} \quad (1)$$

3.1 Modelling strategy

The digital twins presented in the previous section are based in the successive multiplications of Homogeneous Transformation Matrices that represent the kinematics of the specific machine [4]. Translation and rotation of machine axes are included in these transformations, as well as the small displacement and rotation due to different error sources [3].

3.2 Machine model

A key element to the success of the optimization procedure presented here is the proper definition of the model that will represent a realistic behaviour of the machine to be calibrated. The magnitude of each error, their shape, how fast they change within the workspace, the relevance of thermal and flexibility errors determines aspects such as the number of measurements needed or the complexity of the compensation model. The experience and engineering judgement is thus important for defining a proper machine model.

In this work, an approach based on the combination of finite element (FE) model simulation results and synthetically generated geometric errors will be used.

3.3 FE modelling

The goal of the FE modelling and simulation is to obtain the flexibility behaviour of the machine under the influence of gravity. The interaction between the column (Z axis) and the ram (Y axis) in different axes positions will play a major role in this aspect, as non-rigid body behaviour is expected in this type of machines. This "cross-effect" between axes is described in [5].

A model of a real milling machine has been developed [6]. ANSYS software has been used to perform the simulations and the interfaces between moving parts of the machine has been modelled in a way that relative movement is allowed between them. A 9x15x13 3D point grid has been defined covering the machine volume, positioning the 3 linear axes of the machine in each of them. A static structural simulation has been carried out at each axis position, taking the influence of the gravity under consideration, and the deviations of the Tool Center

Point (TCP) have been obtained in each case. This effect is incorporated to machine model M with an interpolated 3D error grid.

3.3.1 Synthetic polynomial errors

In addition to the errors described in the previous section, synthetically generated polynomic errors have been included in the machine model. These errors intend to reflect the effects that cannot be simulated in a FEM model, i.e., guideways and carriage shape errors, scale errors and other local effects. These errors on individual machine components are expanded to the TCP in the form of positioning, straightness and angular errors.

These geometric errors of the machine have been modelled based on orthogonal Legendre polynomials, which are properly suited to model the characteristic shapes of such errors [7]. Equation 2 shows an example of the positioning error of the X axis and equation 3 shows the definition of orthogonal Legendre polynomials.

$$EXX(x) = a_0 \cdot L_0(\bar{x}) + a_1 \cdot L_1(\bar{x}) + \cdots + a_n \cdot L_n(\bar{x}) \quad (2)$$

$$L_n(x) = \frac{1}{2^n n!}\frac{d^n}{dx^n}(x^2\text{-}1)^n \quad (3)$$

a_0, to a_n are the model parameters of order n for each error component, and $\bar{x}$ is the axis position, here normalized to [-1,1] range. L_n represents the Legendre polynomial of order n. The model is defined here by assigning a uniform probability distribution to each parameter variation range (e.g. $[-a_0, a_0]$).

3.3.2 Evaluation of the volumetric error

The volumetric error distribution VE_i is used as the evaluation criteria for the resulting accuracy of the virtual machine model. It is defined here as the difference between the virtual machine model *M* and the same model with all error parameters E_M set to 0 (i.e. an 'ideal' machine), evaluated in a set of X_i machine positions (60x20x20 in this work) distributed over the workspace:

$$VE_i = \|M(X_i, t, E_C)\text{-}M(X_i, t, 0)\| \quad (4)$$

The volumetric error *VE* is defined here as the rms value of the volumetric error distribution VE_i, and it is used as a measure of the global errors of the machine. By performing Monte Carlo simulations on different combinations of the families of machines defined by the parametric digital twin *M*, the probability distribution for the volumetric error distribution VE_i characterizing this family of machines is obtained (see Figure 2). A volumetric error of 11.9 micrometres is obtained. In Figure 2 resulting volumetric error VE_i is evaluated in the machine's XY plane.

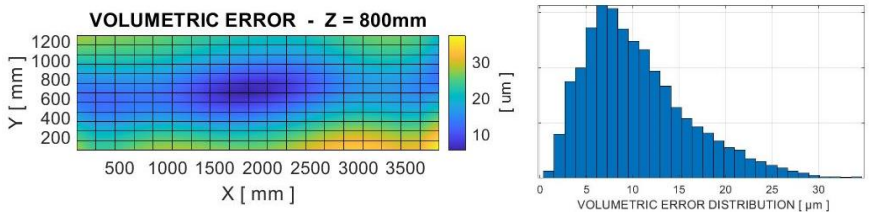

Figure 2. Left: VE_i Volumetric error of a machine model M in XY plane at Z=800. Right: Distribution of the volumetric error VE_i.

3.4 Compensation model

The compensation model *C* has a similar structure as the virtual machine model M. A 21 geometric error rigid-body model is used [8], where each of the errors to identify is approximated by parametric functions defined by Legendre polynomials described in equations 2 and 3. The influence of these errors is incorporated in C with transformation matrices previously described.

In addition to the rigid body model, extra parameters are needed to characterize the cross-effect between Z and Y axes described in section 3.3. For this purpose, 2 additional polynomials are incorporated to the compensation model C. Figure 3 shows a simplified model of the column-ram set, where both elements are modelled as 1 dimensional beams. The column is fixed to the base and the ram transmits a moment due to its own weight, depending on Y position (horizontal), while the application point depends on Z position (vertical).

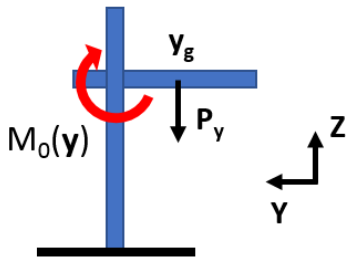

Figure 3. Schematic view of the cross-effect between column and ram.

Following this model, two component errors of the Z axis will be affected by the Y axis: The straightness in Y direction (EYZ) and the rotation around X (EAZ). Applying mechanics of materials principles equations 5 and 6 are obtained for the displacement EYZ and angle EAZ at the joint. Both expressions can be converted to a parametric second and first order polynomials of Z respectively, multiplied by the Y axis. The expressions are shown in equations 5 and 6.

$$E_{YZ} = \frac{-M_0(y)\cdot z^2}{2EI} \rightarrow E_{YZ}(\mathrm{y},\mathrm{z}) = (b_0 + b_1 \cdot \boldsymbol{z} + b_2 \cdot \boldsymbol{z}^2) \cdot \boldsymbol{y} \quad (5)$$

$$E_{AZ} = \frac{-M_0(y)\cdot \mathbf{z}}{EI} \rightarrow E_{AZ}(\mathrm{y},\mathrm{z}) = (\mathrm{c}_0 + c_1 \cdot \boldsymbol{z}) \cdot \boldsymbol{y} \quad (6)$$

Both parametric equation are incorporated to the compensation model C, where the parameters b_n and c_n are going to be estimated in the error minimization process.

4 Model of the error mapping procedure

The error mapping method is based on measuring the position of the balls of a calibrated artefact with a probe incorporated in the machine head. Since the true distance between each pair of balls is known (within error mapping uncertainty in a coordinate measurement machine), it can be compared to the distances as measured by the machine in different positions to obtain information about the positioning accuracy of the machine. A non-linear least square algorithm is used to identify the geometric errors of the machine.

4.1 Artefact design and uncertainty

A calibrated ball artefact is used as measuring target in the error mapping process. The design of the artefact is mainly defined by the number of balls and the relative position between them.

In this work, a 1500 mm long 1D artefact with 11 balls is taken as a reference for the analysis, and the effects of its design parameters will be discussed. Regarding its design, small variations in the distribution of the balls are considered here, introducing small offsets (misalignment according to angle θ in Figure 4) in their positions, as shown in Figure 4. The parameter θ is selected to create vertical and horizontal offsets, as it is considered a feasible variation that does not need to change ball and ball-holder design. The number of balls, N_b, will be also optimized.

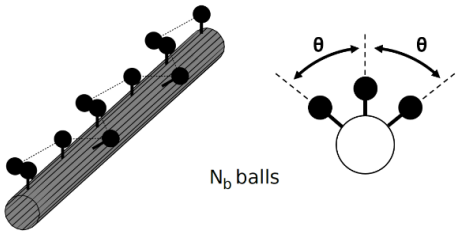

Figure 4. Artefact design according to parameters θ (inclination angle) and N_B (number of balls)

4.2 Artefact position sets

The error mapping process is based on measuring the artefact in several positions to cover the workspace of the machine and provide enough information so that all the parameters of the compensation model can be identified with the expected uncertainty.

Different sets of artefact positions can be considered as base components of the measurement strategy. Direct and indirect measurement approaches should be here differentiated, as each methodology will lead to a substantially different strategies [8].

In this work, a more indirect approach is adopted in order to obtain the machine errors in an efficient way. With this approach automatization or semi automatization of the error mapping process is plausible, if a rotation mechanism is implemented in the centre point, allowing azimuth and elevation rotation. In the next figure, the position sets considered for analysis in this work are represented.

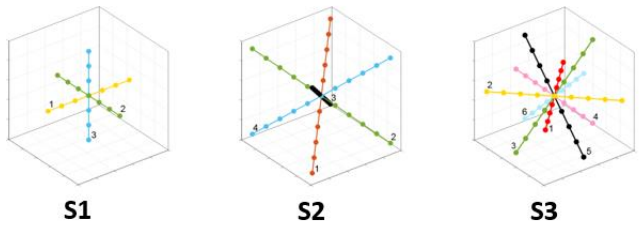

Figure 5. Artefact position sets S1, S2, S3

S1 set includes 3 positions aligned with machines 3 main axes, S2 set consists of 4 position along de 3D diagonals of the machine and the S3 set contains 6 positions crossed in the three main planes (XY, YZ, ZX) of the machine. The artefact position sets do not cover the whole workspace of the machine due to the long travel of the X axis, and therefore more than one set needs to be measured. In this work, the measurement sets are repeated along the X axis to cover the whole workspace.

4.3 Validation criteria

The estimated compensation model *C* is validated by comparing it to the virtual machine model that represents the machine that has been calibrated *M*.

The difference between them defines thus the volumetric compensation error distribution ce_i, and it can be evaluated in a set of X_i machine positions distributed over the workspace, in the same way as in Figure 2:

$$VCE_i = \|C(X_i, t, E_C)\text{-}M(X_i, t, E_M)\| \qquad (7)$$

The volumetric compensated error VCE is defined here as the rms value of the volumetric compensation error distribution $ce_i ce_i$, and it is used as the quality measure of the error mapping process.

5 Optimization of the error mapping procedure

The use of the virtual error mapping optimization procedure presented above is demonstrated here by performing some analysis on the machine and error mapping procedure presented in previous sections. The following design

parameters have been analysed: the number of balls N_b, the ball misalignment according to angle θ and the artefact position set S.

5.1 Artefact design

The optimization procedure is applied here to the optimization of the design of the artefact.

5.1.1 Number of balls

The number of balls in the artefact increases the measurement time but adds measured distances and spatial resolution to the measurement. The nominal value of eleven balls leads to an axial distance between the balls of 150 mm. The artefacts with other number of balls are created keeping the total length of 1500 mm, and thus changing the distance between them. The error mapping and compensation procedure is simulated for seven artefact designs, and their reduction in volumetric error, as defined in Section 4.3, is shown in Figure 6.

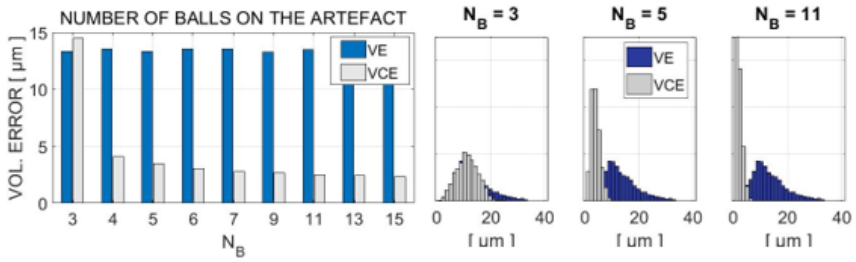

Figure 6. Volumetric error in function of number of balls Nb, for machine M (VE) and C (VCE). Error distribution is shown for cases 3, 5 and 11.

As expected, the error is reduced with higher number of balls, but the improvement is less significant when this number increases. Considering the longer measurement time, a value of 7 balls will be considered optimal in this case, as 95% of the error improvement is obtained and the time cost of adding more positions is considered inefficient.

Figure 7 shows the trajectory estimation of C for several ball number cases, evaluating the error in a Z axis linear trajectory. Significant improvement in machine trajectory estimation can be observed.

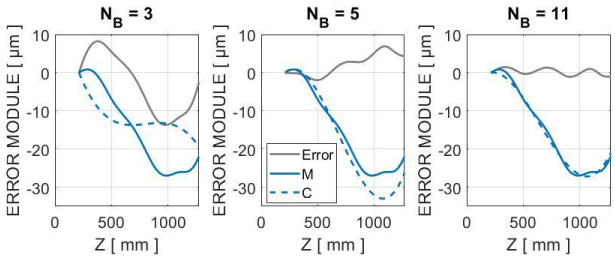

Figure 7. Trajectory estimation along Z of compensation model C (dash blue) compared to machine model M (blue). Cases for NB 3, 5 and 11 are shown.

5.1.2 Ball misalignment

The next analysis looks at the horizontal and vertical offset in the position of the spheres that is generated tilting alternate balls with angle θ along the longitudinal axis of the artefact. Seven different values have been simulated.

For the analysis, strategies S2 and S2+S3 has been used, measuring the 4 main diagonals for the first case, and adding the 6 face-diagonals for the second (see Figure 5). Results are shown in Figure 8.

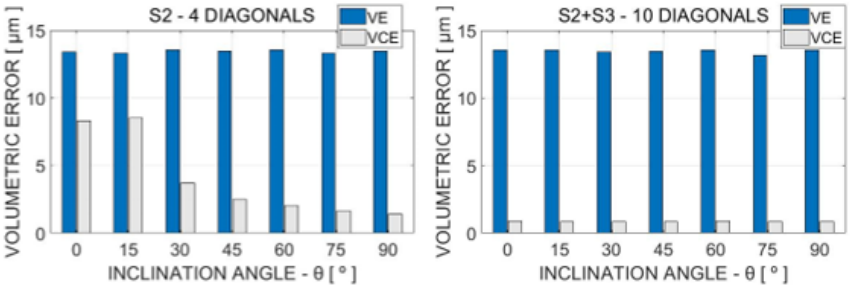

Figure 8. Volumetric error (VE) and compensated error (VCE) in function of the inclination angle θ. Results for S2 (left) and S2+S3 (right) strategies are shown

The simulations show that misalignment of the ball array has almost no effect for the S2+S3 measurement strategy. On the contrary, with a less dense measurement strategy like S2 significant improvement is achieved. In general, it can be seen that with greater misalignment, better volumetric error improvement is achieved, and that this misalignment can allow a lower number of measurements.

5.2 Measurement strategy

Three basic sets have been analysed (see Figure 5), together with all their combinations, and the compensation error and the measurement time have been considered for a fair comparison.

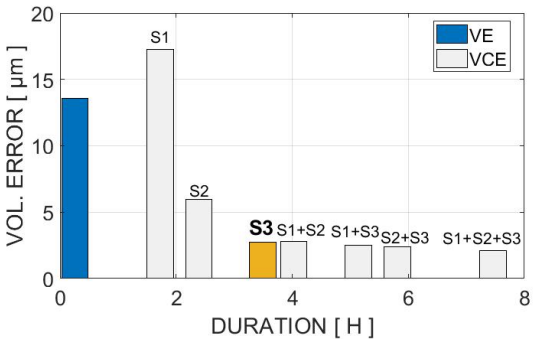

Figure 9. VE and VCE in function of the artefact position set and time. Selected optimal strategy S3 is highlighted.

These results are not so predictable and show how the procedure proposed in this work can help in finding the best result between several, in principle, reasonable approaches, with large differences in measurement time and in the compensation error. S3 could be considered here as an optimal approach.

6 Conclusions

An optimization procedure for artefact-based error mapping processes for a large 3 axis machines has been presented. The procedure allows the optimization of the error mapping procedure, considering aspects such as the design of the artefact, or the positions in the workspace where it is measured.

The procedure has been applied on a large milling machine tool, and some analyses have been performed. The relevance of performing such analysis to ensure that error mapping uncertainty and machine occupation time are optimized has been demonstrated. The obtained criteria are valid for the machine that has been simulated, and the analysis should be performed whenever a new machine is addressed, since the optimal procedure will always depend on the characteristics of the machine and the requirements of the application. With these considerations in mind, some conclusions can be drawn from the performed analysis.

The shape of the artefact, represented here as a misalignment of the balls, helps in reducing mapping uncertainty when a reduced number of measurements is performed.

The optimal number of balls in the artefact or the measurement strategy will depend on the expected uncertainty and available measurement time. Sufficiently good estimations for fast machine verification can be obtained in reduced measurement sets.

7 References

[1] McKeown PA, Loxham J. Some aspects of the design of high precision measuring machines. CIRP Annals 1973;22.
[2] Sartori S, Zhang GX. Geometric Error Measurement and Compensation of Machines. CIRP Annals - Manufacturing Technology 1995;44:599–609.
[3] Aguirre G, Iñigo B, Cilla J, Urreta H. Optimal design of artefacts for machine tool calibration. Euspen 19th International Conference 2019.
[4] Lamikiz A, López de Lacalle LN, Ocerin O, Díez D, Maidagan E. The Denavit and Hartenberg approach applied to evaluate the consequences in the tool tip position of geometrical errors in five-axis milling centres. Int J Adv Manuf Technol 2008;37:122–39.
[5] Ibaraki S, Hiruya M. Assessment of non-rigid body, direction- andvelocity-dependent error motions and their cross-talk by two-dimensional digital scale measurements at multiple positions. Precision Engineering 2020;66:144–53.
[6] Iñigo B, Colinas-Armijo N, Lopez de la Calle LN, Aguirre G. Ambient temperature effect on the volumetric error of a large milling machine. Euspen Thermal Issues n.d.
[7] Haitjema H. Straightness, flatness and cylindricity characterization using discrete Legendre polynomials. CIRP Annals 2020;69:457–60.
[8] Schwenke H, Knapp W, Haitjema H, Weckenmann A, Schmitt R, Delbressine F. Geometric error measurement and compensation of machines–An update. CIRP Annals - Manufacturing Technology 2008;57:660–75.